analytical chemistry

Article

pubs.acs.org/ac

Bovine Serum Albumin-Based Probe Carrier Platform for Electrochemical DNA Biosensing

Yin-Huan Liu,[†,‡,∥] Hong-Na Li,[†,‡,∥] Wei Chen,*[,†,‡] Ai-Lin Liu,[†,‡] Xin-Hua Lin,*[,†,‡] and Yuan-Zhong Chen*[,§]

[†]Department of Pharmaceutical Analysis and [‡]Nano Biomedical Technology Research Center, Fujian Medical University, Fuzhou 350004, China

[§]Fujian Institute of Hematology, Affiliated Union Hospital of Fujian Medical University, Fuzhou 350001, China

Supporting Information

ABSTRACT: A bovine serum albumin (BSA)-monolayer-based probe carrier platform is shown to improve the performance of a conventional thiolated single-stranded DNA probe self-assembled-monolayer-based electrochemical DNA hybridization biosensor. A detection limit of 0.5 fM can be obtained in a very reproducible manner (relative standard deviation <5%), along with high specificity. The performance of the biosensor can be attributed primarily to the enhanced spatial positioning range and accessibility of the probes on the BSA-based platform. Furthermore, the novel biosensor shows high resistance to nonspecific adsorption of nucleic acid and protein and can be directly employed in detection in biological fluids. These advantages give this simple developed methodology great promise for a wide range of nucleic acid testing.

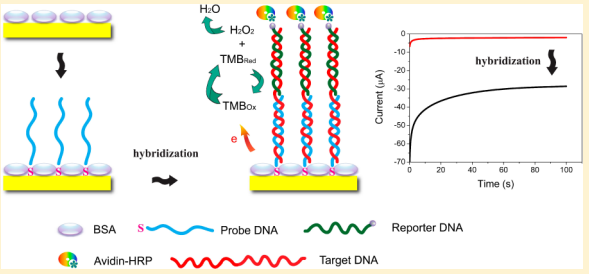

DNA biosensors have attracted a great deal of attention due to their simplicity, speed, and economical assays for gene analysis and testing.[1] They have a broad range of potential applications, including DNA diagnostics, gene analysis, fast detection of biological warfare agents, and forensic applications. Electrochemistry is a promising transduction strategy often employed to develop DNA biosensors due to its high sensitivity, small dimensions, low cost, and compatibility with micromanufacturing technology.[2−13] As compared to other signal transduction methods, the electrochemistry-based approaches should be more appropriate for on-site testing with portable analyzers.

The core of DNA sensing technology is surface-confined single-stranded DNA (ssDNA) probes that are tethered to a substrate for recognition of their complementary DNA target sequence by hybridization. The immobilization of the single-stranded probe on the surface of the electrode dictates the performance of the resulting sensor. Depending on the application, the choice of the immobilization technique is extremely important. A large portion of reported electrochemical DNA sensors are constructed on the basis of self-assembly of thiol-derivatized ssDNA probes on gold surfaces via Au−S chemistry and following passivation by an alkanethiol to backfill the unoccupied space.[14] Unfortunately, it is practically impossible to precisely control the DNA spatial orientation and position on solid surfaces via formation of the self-assembled monolayer (SAM) using thiolated ssDNA molecules.[15−18] Therefore, one often experiences irreproducibility in detection signals. To overcome this, some new platforms such as cone-shaped dendrons,[16] ternary surface monolayers,[18,19] Au nanoparticles on horizontally aligned single-walled carbon nanotubes,[20] tetrahedron-structured DNA probes,[21,22] and "clickable" interfaces on boron-doped diamond electrodes[23,24] have been devoted to control the spatial arrangement of the probe molecules. Despite their many positive attributes, these approaches, however, typically require complex reagents and time-consuming, multistep processing.

In this study, we design a bovine serum albumin (BSA)-based DNA probe carrier platform to better control the interprobe and probe−target interactions on surfaces. The establishment process of the platform is relatively facile and time-saving. Reproducibility and sensitivity of the electrochemical DNA biosensor based on this platform are significantly improved. An extremely low detection limit of DNA target (0.5 fM) can be obtained in a reproducible manner, along with high specificity.

EXPERIMENTAL SECTION

Materials. Bovine serum albumin was obtained from Roche Diagnostics (Mannheim, Germany) and used without further purification. All oligonucleotides were synthesized and purified by TaKaRa Inc. (Dalian, China), and the sequences are (probe) 5′-SH-$(CH_2)_6$-T_{10} CTTCA GAACT GCTGC TCTGG GTCTC AATGG-3′, (reporter) 5′-CTGCC TCCCC GGCGC CACTG GCCAC GTGGT-biotin-3′, (target) 5′-ACCAC GTGGC CAGTG GCGCC GGGGA GGCAG

Received: September 14, 2012
Accepted: December 5, 2012
Published: December 5, 2012

   dx.doi.org/10.1021/ac303397f | Anal. Chem. 2013, 85, 273−277

CCATT GAGAC CCAGA GCAGC AGTTC TGAAG-3′, (single mismatched) 5′-ACCAC GTGGC CAGTC GCGCC GGGGA GGCAG CCATT GAGAC CCAGA GCAGC AGTTC TGAAG-3′, (noncomplementary) 5′-CGGCA AACCA GTCAC ATATA AAATT CCATC AGTCG CTATG GGTCT CTTAG TCGGA AACCT-3′, (PML partial sequence) 5′-ACCAC GTGGC CAGTG GCGCC GGGGA GGCAG AGGAA CGCGT TGTGG TGATC AGCAG CTCGG-3′, and (RARα partial sequence) 5′-TTAGT GGATA TAGCA CACCA TCCCC AGCCA CCATT GAGAC CCAGA GCAGC AGTTC TGAAG-3′. The 3,3′,5,5′-tetramethylbenzidine (TMB) substrate (Neogen K-blue low-activity substrate) was from Neogen (Lansing, MI). Avidin−horseradish peroxidase (HRP) was from Roche Diagnostics. The buffer solutions used in this study were as follows: The DNA immobilization buffer contained 10 mM Tris−HCl, 1 mM ethylenediaminetetraacetic acid, and 1 M NaCl (pH 8.0). The hybridization buffer was a 10 mM phosphate buffer (PB) solution containing 1 M NaCl (pH 7.4). All solutions were prepared with Milli-Q water (18 MΩ cm resistivity) from a Millipore system.

Electrochemical Detection. An electrochemical analyzer (CHI 660C, CH Instruments, Austin, TX) was used for the amperometric and cyclic voltammetry (CV) experiments and was connected to a conventional Au disk working electrode (2 mm diameter), a Ag/AgCl reference electrode, and a Pt wire auxiliary electrode. CV was carried out at a scan rate of 100 mV/s. The surface density of DNA sequences was determined by the chronocoulometric method.[25] The chronocoulometric plots (charge vs square root of time) of the DNA recognition surface were obtained in 10 mM Tris−HCl (pH 7.4) buffer. Cationic redox-active hexaammineruthenium(III) ($[Ru(NH_3)_6]^{3+}$) (50 μM) was then introduced into the buffer solution and allowed to equilibrate for 1 min followed by chronocoulometric measurement. The surface coverage of $[Ru(NH_3)_6]^{3+}$ was calculated as the difference in the chronocoulometric intercepts in the absence and presence of $[Ru(NH_3)_6]^{3+}$ and converted to the DNA surface density using the relationship $\Gamma_{DNA} = \Gamma_0(z/m)N_A$, where Γ_{DNA} is the surface density of the DNA, Γ_0 is the surface coverage of $[Ru(NH_3)_6]^{3+}$, z is the charge of $[Ru(NH_3)_6]^{3+}$, m is the number of DNA bases, and N_A is Avogadro's number.

Preparation of the BSA-Based Biosensor. The gold electrode was cleaned following the reported protocol.[26] The cleaned electrode was incubated with 5 mg/mL BSA in 10 mM PB (pH 7.4) at open-circuit potential for 15 min at room temperature. A 4 μL volume of 1 μM probe DNA solution was drop cast to cover the BSA-modified gold electrode and incubated for 1 h at room temperature. Finally, the sensor was thoroughly rinsed with water and dried under nitrogen.

DNA Hybridization Assay. The DNA detection protocol involved a sandwich-type hybridization assay and the capture of the HRP enzyme tag. Different concentrations of the DNA target were mixed with the biotinylated reporter probe (20 nM) in the hybridization buffer. A 4 μL volume of this target/reporter hybrid solution was cast onto the electrode surface and incubated for 50 min at 50 °C. The electrode was then rinsed with water and incubated with 2 mL of avidin−HRP (0.5 U/mL) for 15 min at room temperature. Finally, the sensor was extensively rinsed and subjected to electrochemical measurements. Amperometric detection was performed in TMB substrate (Neogen K-blue low-activity substrate) with a fixed potential of 0 V, and the current was sampled at 100 s.

RESULTS AND DISCUSSION

Sensing Strategy. The principle of the BSA-based DNA probe carrier platform for electrochemical DNA biosensing is outlined in Scheme 1. BSA molecules are first self-assembled on the Au electrode to form a porous monolayer. Thiolated ssDNA probes are immobilized in the interval of BSA molecules. In the presence of target DNA and biotin-labeled reporter DNA, hybridization forms the sandwich structure. Avidin−HRP is further attached to the sandwich structure via biotin−avidin conjugation as an enzymatic label. The enzymatic label HRP can catalyze the redox reaction between H_2O_2 and TMB. The electrochemical reduction current of oxidized TMB is used to quantify the effects of complementary bases.

Scheme 1. Schematic Illustration of the BSA-Based DNA Probe Carrier Platform for Electrochemical DNA Biosensing

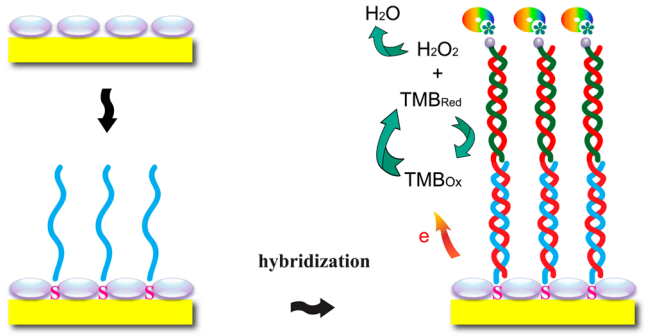

Bovine Serum Albumin-Based Probe Carrier Platform. Bovine serum albumin has been described as an ellipsoidal molecule with hydrodynamic dimensions of 14 × 4 × 4 nm.[27] Earlier studies have shown that albumin can adsorb strongly on various metals.[28−31] A monolayer of horizontally adsorbed albumin on a gold surface can be achieved at open-circuit potential and physiological pH according to the radiolabeling investigation.[28] The expected horizontal orientation of BSA has also been proved by electrochemical quartz crystal nanobalance (EQCN) measurements and atomic force microscopy (AFM) analysis.[29] In this work, the protein adsorption process was monitored by cyclic voltammetry according to a previous report.[28] Figure 1 shows successive cyclic voltammograms in potassium ferricyanide before (bare electrode) and after

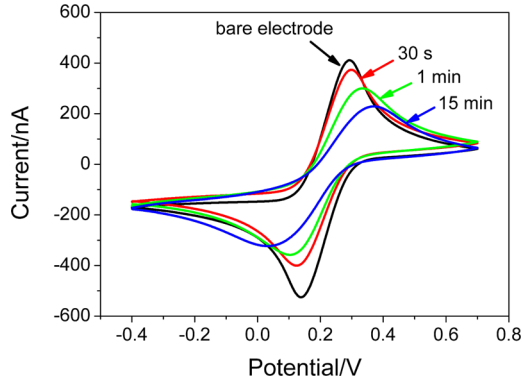

Figure 1. Comparison of cyclic voltammograms recorded on a gold electrode after adsorption of BSA (5 mg/mL, pH 7.4) at open-circuit potential. Cyclic voltammograms were recorded in a solution of 10 mM $K_3Fe(CN)_6$ containing 0.1 M KCl. Scan rate 100 mV/s.

dx.doi.org/10.1021/ac303397f | Anal. Chem. 2013, 85, 273−277

exposure to solutions of 5 mg/mL BSA prepared in 10 mM PB (pH 7.4) at open-circuit potential for various lengths of time. Within 15 min, the anodic and cathodic peaks broaden as the adsorption time increases, and the peak currents decrease at the same time. The above changes in the cyclic voltammograms are brought about by a decrease in the electron transfer rate constant of ferricyanide due to the electrode surface becoming coated with a negatively charged protein layer. This layer acts as a barrier preventing the ferricyanide anions from approaching the electrode surface. The appearance of the plateau region of the peak current and redox peak potential difference after 15 min indicates that at longer adsorption times no further reduction in electron blocking occurs. The remaining redox probe signal is less than 40% of the initial unperturbed signal, but it does not vanish completely, indicating the existence of uncovered surface area under the porous BSA layer, which is accessible to the probe ions.

To further examine the porosity of the protein film and at the same time evaluate the viability of constructing an electrochemical DNA sensor using BSA-decorated gold electrodes, the electron transfer reactivity of TMB at the BSA-conjugated surface was investigated. Interestingly, we found that TMB exhibited an electrochemical response at the BSA-modified surface similar to that at the bare gold electrode (Figure 2). The

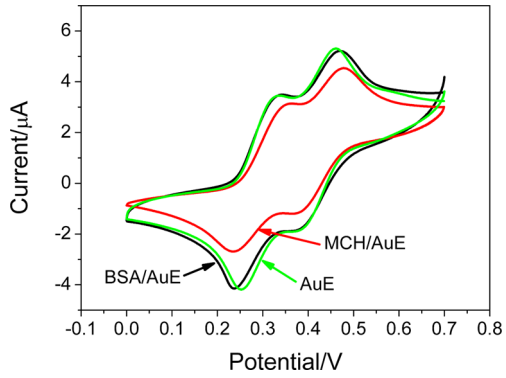

Figure 2. Cyclic voltammograms of TMB recorded on a gold electrode (AuE), BSA-modified gold electrode (BSA/AuE), and MCH-modified gold electrode (MCH/AuE). Scan rate 100 mV/s.

electrochemical response was significantly higher than that at the mercaptohexanol (MCH)-modified surface, suggesting that TMB could easily penetrate the hollow structures comprising the BSA layer and an enhanced signal could be obtained in the biosensing process. A charge effect, which results in the different electrochemical responses of ferricyanide and TMB on the BSA-modified electrode, can be proved by using hexaammineruthenium(III) chloride as the redox probe (see the Supporting Information, Figure S1).

The probe DNA immobilization process is the most time-consuming step in the preparation of the conventional thiolated ssDNA probe SAM-based electrochemical biosensor (overnight at 4 °C). However, the optimized recognition interface established on the BSA-based probe carrier platform can be achieved within 1.5 h, which is less than one-sixth of that used for establishment of the conventional thiolated ssDNA probe SAM-based electrochemical biosensor. As shown in Figure 3, the response signal of the biosensor increased with the assembly time of the probe and reached a plateau at 1 h. The probe density on the BSA-based platform was determined by chronocoulometry to be 1.66×10^{12} molecules/cm^2, which

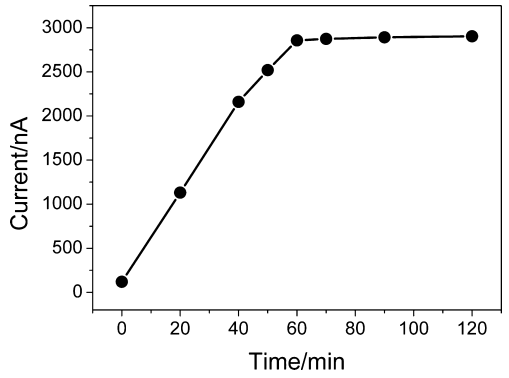

Figure 3. Influence of the assembly time of probe DNA on the amperometric response of the biosensor.

was very consistent with the coverage of the BSA monolayer with a flat orientation and close packing (1.76×10^{12} molecules/cm^2). This implies that the thiolated DNA probes are immobilized on the gold surface in the interval of BSA molecules. In addition, passivation by alkanethiol is unnecessary for the BSA-based probe carrier platform. This simplifies the establishment process of the biosensor further.

Performance of the Biosensor. In the development and practical application of the electrochemical biosensor, one of the critical issues is the reproducibility of the testing results. Up to now, most of the research on DNA biosensors has been focused on the improvement of the sensitivity and specificity. A reproducible result for nucleic acid detection is still the main challenge for electrochemical gene sensors. In conventional electrochemical DNA biosensors, the assembly of the probes, especially the spatial distribution of the probes, is considerably random. Biosensors with similar probe amounts, which are fabricated under the same conditions, exhibit quite different electrochemical responses to the target sequence. As shown in Figure 4, the electrochemical response varied widely for the DNA biosensor based on conventional thiolated probe self-assembly and mercaptohexanol passivation. The relative standard derivation of eight independent tests for 10 nM target sequence was 27.2%. This indicates that the hybridization efficiency is not controllable at the HS-DNA SAMs due to the irregular spacing between probe DNA molecules. Our strategy to design and construct recognition probes on a BSA-based platform provides a significantly enhanced spatial positioning range and accessibility of the probes on a surface. Very reproducible electrochemical responses can be achieved in this case. The relative standard derivation of eight independent tests for 1 and 10 nM target sequence was 2.6% and 4.0%, respectively.

As also can be seen from Figure 4, the novel biosensor we established is more sensitive than the conventional one. This can be ascribed to the probe density being a controlling factor for the efficiency of target capture as well as for the kinetics of the target/probe hybridization.[32] The hybridization efficiency of the probes in the presence of 10 nM target sequence determined by chronocoulometry increased from 15.5% to 91.4% when the BSA-based probe carrier platform was used.

The applicability of the new genosensor was illustrated for measuring the promyelocytic leukemia/retinoic acid receptor α (PML/RARα) fusion gene in acute promyelocytic leukemia (APL). We challenged the sensor with the synthetic DNA target of a series of concentrations across the range of 0.01 pM to 10 nM. As shown in Figure 5A, the amperometric signal

dx.doi.org/10.1021/ac303397f | Anal. Chem. 2013, 85, 273−277

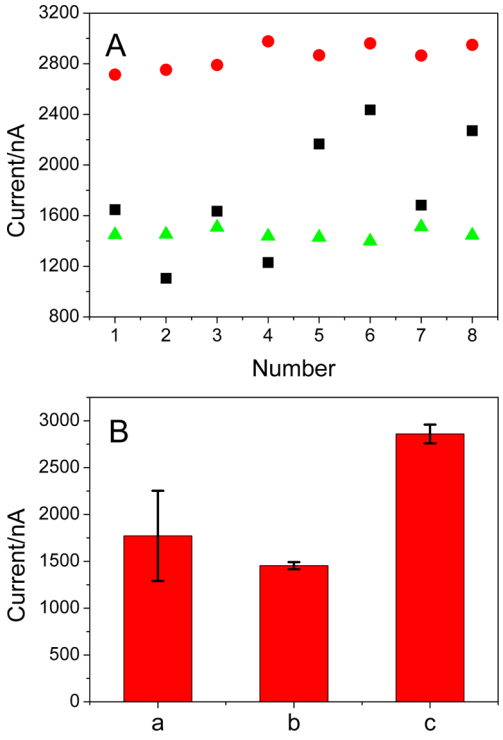

Figure 4. (A) Amperometric responses of eight independent tests for 10 nM target sequence on ssDNA/MCH/AuE (■), 1 nM target sequence on ssDNA/BSA/AuE (▲), and 10 nM target sequence on ssDNA/BSA/AuE (●). (B) Bar graph corresponding to the amperometric responses obtained with (a) 10 nM target sequence on ssDNA/MCH/AuE, (b) 1 nM target sequence on ssDNA/BSA/AuE, and (c) 10 nM target sequence on ssDNA/BSA/AuE. Error bars show the standard deviations of measurements taken from eight independent experiments.

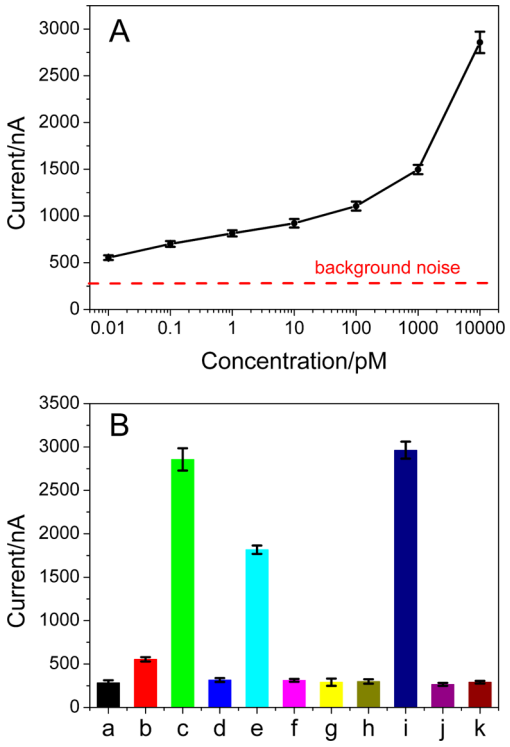

Figure 5. (A) Amperometric signal vs logarithmic concentration of the target DNA. (B) Bar graph corresponding to the amperometric responses obtained with (a) 0 nM target DNA, (b) 10 fM target DNA, (c) 10 nM target DNA, (d) 10 nM noncomplementary oligonucleotide, (e) 10 nM single-base-mismatched oligonucleotide, (f) HRP, (g) 20 nM reporter probe, (h) 0 nM target DNA in the presence of 25% serum, (i) 10 nM target DNA in the presence of 25% serum, (j) 10 nM PML partial sequence, and (k) the RARα partial sequence. Error bars show the standard deviations of measurements taken from at least three independent experiments.

increased nonlinearly with the logarithmic concentration of the target, spanning an impressive response region of 7 orders of magnitude. A detection limit of 0.5 fM, which corresponds to 2 zmol in the 4 μL sample, could be estimated using 3σ (where σ is the standard deviation of the blank solution, n = 8). Even without rigorous signal amplification, this BSA-platform-based sensor is much more sensitive than ssDNA probe/MCH-based sensors with similar enzyme-based signal transduction, exhibiting a 500000-fold improvement in the detection limit (0.5 fM vs 250 pM[33]). The specificity of the sensing protocol was examined by challenging the system with noncomplementary and mismatched oligonucleotides. As expected, noncomplementary oligonucleotides display a negligible change in the response to the control signal without the nucleic acid (Figure 5B). The single-base-mismatched DNA yields a smaller defined signal as compared to that observed for a similar target concentration, reflecting the partial duplex formation of the single mismatch. Moreover, a significant current increment can be observed even in the presence of 10 fM PML/RARα fusion gene, but no significant difference of current could be observed for ssDNA and its hybridization with 10 nM partial PML and partial RARα, making it possible for this protocol to distinguish APL patients from healthy people. At the same time, the BSA-based probe carrier platform shows significantly high resistance to the nonspecific adsorption of nucleic acid and of protein (such as the HRP tag). To also evaluate the applicability of the new electrochemical genosensor to biological fluids, we have compared its performance in pure hybridization buffer and in complex biological samples. Significantly, we found that the BSA-based sensor was highly resistant to serum, with minimal alteration of the background noise and nearly the same hybridization signal for the 10 nM target even in the presence of 25% human serum. These results suggest that the presence of biological fluids has little effect on the performance of the sensor, indicating great potential for real-world applications.

■ CONCLUSIONS

In summary, we have reported a BSA-based platform for immobilization of nucleic acid probes on gold surfaces. The electrochemical DNA biosensor based on the novel probe carrier platform provides several unique features which lead to a significantly improved performance compared to that of the conventional thiolated DNA probe SAM approach. Bovine serum albumin is used in the conventional method for preventing nonspecific adsorption of protein. Therefore, no additional reagent is required in our method. In addition, passivation by alkanethiol is unnecessary for the BSA-based probe carrier platform, which simplifies the establishment process of the biosensor. The BSA-based probe carrier platform can be achieved in 15 min. Meanwhile, the probe immobilization on the BSA-based platform with well-controlled spacing can be fulfilled in 1 h, which is a lot of time-savings as compared to the process for other thiolated ssDNA probe SAM-based electrochemical biosensors. Because of the high protein resistance ability, BSA-based sensors can be directly

dx.doi.org/10.1021/ac303397f | Anal. Chem. 2013, 85, 273−277

employed in detection in biological fluids. More significantly, an enhanced spatial positioning range and accessibility of the probes on the BSA-based platform result in excellent reproducibility and high detection sensitivity. These advantages make this probe carrier platform a new paradigm in biosensor design.

■ ASSOCIATED CONTENT

Supporting Information

Cyclic voltammograms of $[Ru(NH_3)_6]^{3+}$. This material is available free of charge via the Internet at http://pubs.acs.org.

■ AUTHOR INFORMATION

Corresponding Author

*E-mail: chenandhu@163.com (W.C.); xhl1963@sina.com (X.-H.L.); chenyz@pub3.fz.fj.cn (Y.-Z.C.).

Author Contributions

‖These authors contributed equally to this work.

Notes

The authors declare no competing financial interest.

■ ACKNOWLEDGMENTS

We gratefully acknowledge the financial support of National High Technology and Development of China (863 Project 2012AA022604), the National Natural Science Foundation of China (Grant 21175023), the Natural Science Foundation of Fujian Province (Grants 2011J01034 and 2012J06019), the Science and Technology Planning Project of Fujian Province (Grant 2011Y0030), and the Program for New Century Excellent Talents in Fujian Province University (Grant JA11102).

■ REFERENCES

(1) Sassolas, A.; Leca-Bouvier, B. D.; Blum, L. J. *Chem. Rev.* **2008**, *108*, 109−39.

(2) Lin, L. Q.; Liu, Q. C.; Wang, L. M.; Liu, A. L.; Weng, S. H.; Lei, Y.; Chen, W.; Lin, X. H.; Chen, Y. Z. *Biosens. Bioelectron.* **2011**, *28*, 277−283.

(3) Bonanni, A.; Pumera, M. *ACS Nano* **2011**, *5*, 2356−2361.

(4) Zhang, J.; Song, S.; Wang, L.; Pan, D.; Fan, C. *Nat. Protoc.* **2007**, *2*, 2888−2895.

(5) Shiddiky, M. J. A.; Torriero, A. A. J.; Zeng, Z.; Spiccia, L.; Bond, A. M. *J. Am. Chem. Soc.* **2010**, *132*, 10053−10063.

(6) Lin, L. Q.; Chen, J.; Lin, Q. H.; Chen, W.; Chen, J. H.; Yao, H.; Liu, A. L.; Lin, X. H.; Chen, Y. Z. *Talanta* **2010**, *80*, 2113−2119.

(7) Xia, F.; White, R. J.; Zuo, X.; Patterson, A.; Xiao, Y.; Kang, D.; Gong, X.; Plaxco, K. W.; Heeger, A. J. *J. Am. Chem. Soc.* **2010**, *132*, 14346−14348.

(8) Kannan, B.; Williams, D. E.; Booth, M. A.; Travas-Sejdic, J. *Anal. Chem.* **2011**, *83*, 3415−3421.

(9) Lin, L. Q.; Lin, X. H.; Chen, J. H.; Chen, W.; He, M.; Chen, Y. Z. *Electrochem. Commun.* **2009**, *11*, 1650−1653.

(10) Palecek, E.; Bartosik, M. *Chem. Rev.* **2012**, *112*, 3427−3481.

(11) Zhang, J.; Song, S. P.; Zhang, L. Y.; Wang, L. H.; Wu, H. P.; Pan, D.; Fan, C. H. *J. Am. Chem. Soc.* **2006**, *128*, 8575−8580.

(12) Dubuisson, E.; Yang, Z. Y.; Loh, K. P. *Anal. Chem.* **2011**, *83*, 2452−2460.

(13) Liu, A. L.; Wang, K.; Weng, S. H.; Lei, Y.; Lin, L. Q.; Chen, W.; Lin, X. H.; Chen, Y. Z. *TrAC, Trends Anal. Chem.* **2012**, *37*, 101−111.

(14) Herne, T. M.; Tarlov, M. J. *J. Am. Chem. Soc.* **1997**, *119*, 8916−8920.

(15) Lao, R. J.; Song, S. P.; Wu, H. P.; Wang, L. H.; Zhang, Z. Z.; He, L.; Fan, C. H. *Anal. Chem.* **2005**, *77*, 6475−6480.

(16) Park, J. Y.; Kwon, S. H.; Park, J. W.; Park, S. M. *Anal. Chim. Acta* **2008**, *619*, 37−42.

(17) Keighley, S. D.; Li, P.; Estrela, P.; Mighorato, P. *Biosens. Bioelectron.* **2008**, *23*, 1291−1297.

(18) Wu, J.; Campuzano, S.; Halford, C.; Haake, D. A.; Wang, J. *Anal. Chem.* **2010**, *82*, 8830−8837.

(19) Henry, O. Y. F.; Perez, J. G.; Sanchez, J. L. A.; O'Sullivan, C. K. *Biosens. Bioelectron.* **2010**, *25*, 978−983.

(20) Li, L.; Wang, S.; Yang, T.; Huang, S. M.; Wang, J. C. *Biosens. Bioelectron.* **2012**, *33*, 279−283.

(21) Pei, H.; Lu, N.; Wen, Y. L.; Song, S. P.; Liu, Y.; Yan, H.; Fan, C. H. *Adv. Mater.* **2010**, *22*, 4754−4758.

(22) Schlapak, R.; Danzberger, J.; Armitage, D.; Morgan, D.; Ebner, A.; Hinterdorfer, P.; Pollheimer, P.; Gruber, H. J.; Schaffler, F.; Howorka, S. *Small* **2012**, *8*, 89−97.

(23) Szunerits, S.; Niedziolka-Jonsson, J.; Boukherroub, R.; Woisel, P.; Baumann, J. S.; Siriwardena, A. *Anal. Chem.* **2010**, *82*, 8203−8210.

(24) Meziane, D.; Barras, A.; Kromka, A.; Houdkova, J.; Boukherroub, R.; Szunerits, S. *Anal. Chem.* **2012**, *84*, 194−200.

(25) Steel, A. B.; Herne, T. M.; Tarlov, M. J. *Anal. Chem.* **1998**, *70*, 4670−4677.

(26) Chen, W.; Liu, Y. H.; Li, H.-N.; Liu, A. L.; Lin, X. H.; Chen, Y. Z. *Anal. Chim. Acta* **2012**, *748*, 89−94.

(27) Mamedova, N. N.; Kotov, N. A.; Rogach, A. L.; Studer, J. *Nano Lett.* **2001**, *1*, 281−286.

(28) Moulton, S. E.; Barisci, J. N.; Bath, A.; Stella, R.; Wallace, G. G. *J. Colloid Interface Sci.* **2003**, *261*, 312−319.

(29) Stobiecka, M.; Hepel, M.; Radecki, J. *Electrochim. Acta* **2005**, *50*, 4873−4887.

(30) Dolatshahi-Pirouz, A.; Rechendorff, K.; Hovgaard, M. B.; Foss, M.; Chevallier, J.; Besenbacher, F. *Colloids Surf.* **2008**, *66*, 53−59.

(31) Desroches, M. J.; Chaudhary, N.; Omanovic, S. *Biomacromolecules* **2007**, *8*, 2836−2844.

(32) Peterson, A. W.; Heaton, R. J.; Georgiadis, R. M. *Nucleic Acids Res.* **2001**, *29*, 5163−5168.

(33) Carpini, G.; Lucarelli, F.; Marrazza, G.; Mascini, M. *Biosens. Bioelectron.* **2004**, *20*, 167−175.